International Journal of Rotating Machinery, 8(3): 185–192, 2002

1023-621X/02 $12.00+.00

A Three Dimensional Modeling of the Dynamic Behavior of Composite Rotors

E. CHATELET*, D. LORNAGE, and G. JACQUET-RICHARDET
INSA de LYON, Laboratoire de Mécanique des Structures, Bâtiment 113, 20, Avenue Albert Einstein, 69100 Villeurbanne, France

Composite materials are now used for many rotor applications and different adapted modeling techniques have been discussed. Analytical approaches or numerical approaches based on beam theories are useful but can be limited by their associated assumptions. On the other hand, a direct finite element discretisation overcomes these limitations but often leads to prohibitive computational costs. The approach proposed here is based on a finite element full modeling associated with two reduction techniques. First the dynamic behavior of the rotating structures is written in terms of mode shapes of the structure at rest. Second the structure is supposed to be cyclically symmetric.

Applications, based on a multilayered shell element, first illustrate and validate the proposed model. Then, a simple disc-shaft assembly is considered and the results obtained point out coupling effects between the flexible parts of the assembly.

Keywords: Composite rotors; Disc-shaft coupling; Dynamic behavior; Effect of rotation

Because of their high strength, high stiffness, and low density characteristics, composite materials are now used widely for the design of rotating mechanical components such as, for example, driveshafts for helicopters, cars and jet engines, or centrifugal separator cylindrical tubes. The interest of composites for rotordynamic applications has been demonstrated both numerically and experimentally (Zorzi & Giordano, 1985; Darlow & Creonte, 1995; Singh et al., 1997; Gupta & Singh, 1998). These materials provide direct advantages in terms of weight saving, placement of critical speeds, smoother and supercritical operations. They also give the designer the possibility to obtain a predetermined behavior, without weight or geometry penalties, by changing the arrangement of the different composite layers: number of plies, orientation ... (Bauchau, 1983).

When the shaft is thick and long, only longitudinal bending deformations need to be considered. On the other hand, when the structure becomes thin-walled, deformations of the sections should also be considered. These deformations have a significant effect on flapwise bending modes and are fully associated with ring-type modes. Thin rotating tubes, used for example in high speed centrifugal separators, have also been intensively analysed (Lam & Loy, 1995; Sun et al., 1997).

The behavior of composite rotors is usually studied using the equivalent modulus beam approach, where equivalent longitudinal and in plane shear moduli are obtained from the classical laminate theory and then used within conventional beam models (analytical or finite element models). This approach, often precise enough, can lead to significant errors when its basic hypotheses are not respected (Singh & Gupta, 1994a). First the laminate theory supposes that the contribution of each layer is independent of its radial position. This assumption is valid for thin walled shafts with symmetrical sequences or for shafts obtained with the filament winding process with a constant winding angle. Second the beam theory supposes that cross sections are not deformed during longitudinal bending. Finally, thickness shear effects are supposed to be negligible. Refined beam theories, obtained by direct reduction from layerwise shell theories, overcome some of the limitations associated with the equivalent modulus beam approach (Dos Reis et al., 1987a; Singh & Gupta, 1996).

Longitudinal bending modes as well as ring modes can be obtained using shell formulations (Smirnov, 1989). Various shell theories, extensively analyzed in the literature

Received in final form 21 May 2000.
*Corresponding author. Fax: 33-472 438 930. E-mail: chatelet@lmst.insa-lyon.fr

have been applied to thin to moderately thick composite shafts (Singh & Gupta, 1994) or to thin-walled tubes (Lam & Loy, 1995). Most of the published studies are based on analytical approaches. A few studies consider also numerical modelisations based on direct finite element discretisations (Chen et al., 1993; Sun et al., 1997) or on discretisations based on axisymmetric finite elements with full Fourier series expansion in the circumferential direction (Padovan, 1975; Stephenson & Rouch, 1993; Sivadas & Ganesan, 1994).

Analytical approaches are useful but unfortunately they can only be derived for a few special lamination and boundary configurations. Furthermore, as axisymmetrical approaches, they cannot be applied when the structure or the loading are not perfectly rotationally uniform. On the other hand, a direct finite element discretisation of the structure overcomes these limitations and allows precise modelings but has three main drawbacks. First, the model should be fine enough inducing often prohibitive computational costs. For example, Sun et al. (1997) showed on a particular application that, for ring modes, about ten elements per half wave should be used in the circumferential direction. Second, the behavior of the structure should not be computed only once, but for a sufficient number of operating points in order to be able to draw the evolution of the dynamic behavior with rotation on a Root Locus diagram. Then, in this case, the consequences of model size are dramatically amplified. Finally, a direct modeling gives all the frequencies in an ascending order. A significant number of frequencies have to be calculated and then classified according to the associated mode shapes.

The approach proposed here is based on a finite element full modeling of the structure but uses two reduction techniques in order to avoid the drawbacks pointed out (Jacquet-Richardet et al., 1996). First, the dynamic behavior of the rotating structure is written in terms of a set of mode shapes associated with the structure at rest. Second, the structure is supposed to be constituted by identical cyclic symmetrical sectors and the behavior of the whole structure at rest is obtained from a finite element model involving only one of these sectors. This procedure, adapted to isolated shafts as well as disc-shaft or wheel-shaft assemblies, leads to considerable computer cost savings and can be used whatever the finite element considered (shell, volume...). Other advantages are that both longitudinal bending and ring-type modes can be obtained at the same time and that, due to the property of cyclic symmetry, mode shapes are automatically pre-classified.

In this paper, the proposed method is first rapidly presented. Then the finite element considered for the applications, which is a multilayered shell element, is described. Four applications are presented. The first three are aimed at validating the method and showing its capacity to deal efficiently with longitudinal bending as well as ring-type modes. The last one considers a simple shaft disc assembly and points out the possible couplings between the two parts of the assembly.

THEORETICAL BACKGROUND

The motion equations, expressed in a body fixed coordinate system, of a flexible assembly rotating at a given uniform angular velocity can be expressed after finite element discretisation as (Jacquet-Richardet et al., 1996):

$$[KE + KG(\{\delta\}_s) - KS]\{\delta\}_s = \{FC(\Omega^2)\} \quad [1]$$

$$[M]\{\ddot{\delta}\}_d + [CM + CR]\{\dot{\delta}\}_d + [KE + KG - KS]\{\delta\}_d = \{0\} \quad [2]$$

where $[M]$ is the mass matrix, $[CM]$ the mechanical damping matrix, $[CR]$ the gyroscopic matrix, $[KE]$ the elastic stiffness matrix, $[KG]$ the geometric stiffness matrix (stress stiffening) and $[KS]$ the supplementary stiffness matrix (spin softening). $\{FC\}$ is the modal centrifugal forces vector, $\{\delta\}_s$ the static equilibrium position under centrifugal loading and $\{\delta\}_d$ the small amplitude dynamic displacement around the static position.

When the structure is constituted by N identical jointed sectors (cyclic symmetry) the size of the problem can be reduced by applying the wave propagation theory in periodic media (Thomas, 1979). In this case, the displacement of the different sectors are related to the corresponding quantities associated with a reference sector, by the following relations:

$$\{\delta\}_d^p = \{\delta_n^c\}\cos(p-1)\beta n + \{\delta_n^s\}\sin(p-1)\beta n \quad [3]$$

where $\{\delta\}_d^p$ is the dynamic displacement of sector p, $\{\delta_n^c\}$ and $\{\delta_n^s\}$ are generalized quantities associated with the basic sector and $\beta_n = 2\pi n/N$ is the phase difference between the displacement of two adjacent sectors. N is the total number of sectors and n, Fourier order, takes the discrete values:

$$\begin{aligned} &n = 0, 1, \ldots, N/2 && \text{if } N \text{ is even} \\ &n = 0, 1, \ldots, (N-1)/2 && \text{if } N \text{ is odd} \end{aligned} \quad [4]$$

Applying the wave propagation relations [3], the dynamic problem [2] is divided into small size systems associated with each of the possible phase angle β_n.

$$[M]_n\{\ddot{\delta}_n\} + [CM_n + CR_n]\{\dot{\delta}_n\} + [KE_n + KG_n - KS_n]\{\delta_n\} = \{0\} \quad [5]$$

where $\{\delta_n\} = \langle \delta_n^c, \delta_n^s \rangle^t$

At rest and without damping [5] reduces to:

$$[M_n]\{\ddot{\delta}_n\} + [KE_n]\{\delta_n\} = \{0\} \quad [6]$$

The solution of [6] gives a set of mode shapes which are grouped into a modal matrix $[\Psi_n]$. Assuming that the mode shapes of the rotating structure can be written as a linear combination of the associated mode shapes of the undamped structure at rest:

$$\{\delta_n\} = [\Psi_n]\{q_n\} \quad [7]$$

system [5] becomes:

$$[m_n]\{\ddot{q}_n\} + [c_n]\{\dot{q}_n\} + [k_n]\{q_n\} = \{0\} \quad [8]$$

with

$$\begin{aligned} [m_n] &= [\Psi_n]^t[M_n][\Psi_n] \\ [c_n] &= [\Psi_n]^t[CM_n + CR_n][\Psi_n] \\ [k_n] &= [\Psi_n]^t[KE_n + KG_n - KS_n][\Psi_n] \end{aligned} \quad [9]$$

The solution of [6] and [8] is performed for all the possible values of the phase parameter $\beta_n = 2\pi n/N$ given by [4]. The frequencies of the rotating system are given directly. The corresponding mode shapes are obtained after applying the two successive transformations [7] and [3] to the calculated eigenvectors.

Shaft modes can occur only with $n=0$ or $n=1$ ($n=0$ torsion and longitudinal modes, $n=1$ bending modes). Ring modes or disc modes are always classified using an analogy with axisymmetric modes which are characterized by nodal diameters and nodal circles. They are either zero ($n=0$), one ($n=1$), two ($n=2$) or more ($n>2$) nodal diameter bending or torsion modes.

According to the proposed analysis method, the non rotating mode shapes of the assembly are calculated only once. Then the following steps are involved for each rotation speed considered:

- The static problem is solved.
- The dynamic problem [5] is reduced according to [7].
- The reduced system [8] is solved.

Compared to traditional procedures, the computer cost saving is considerable and allows precise analyses of complex structures using efficient workstations. The procedure can be shortened if stress stiffening effects are negligible.

APPLICATION – VALIDATION

Finite Element Modeling

The proposed approach can be used whatever the finite element considered. The element chosen here is a multilayered shell element, constructed from the solid isoparametric element with 16 nodes, by applying the Reissner–Mindlin kinematical hypotheses (Ahmad et al., 1970; Jacquet-Richardet & Swider, 1997). The resulting element is geometrically characterized by 16 nodes and cinematically by 8 nodes and 5 degrees of freedom per node (Figure 1).

Matrices are obtained by summation of the contribution of the different layers. As shear strain distribution is assumed constant through the thickness, a shear correction

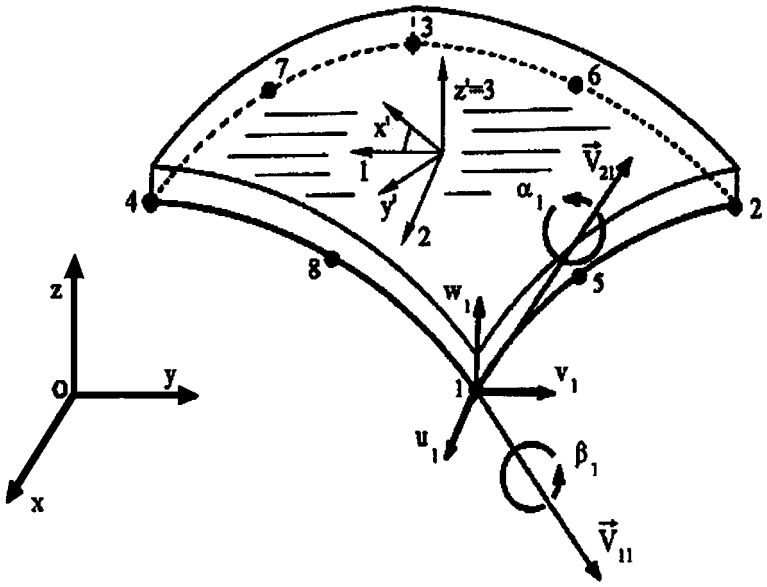

FIGURE 1 Multilayered degenerated solid shell element.

coefficient equal to 5/6 is considered. Reduced integration is used to prevent shear locking.

In the following, three applications are considered in order to validate and illustrate the proposed method. The first considers shaft bending modes and is based on the thin-walled composite shaft first proposed by Zinberg and Symmonds (1970) and considered as a reference test case by a number of authors: Dos Reis et al. (1987b), Bert and Kim (1995), Singh and Gupta (1996). The second considers ring type modes and is based on a simply supported thin-walled cylinder proposed by Sun et al. (1997). The last application is based on the same structure but totally free in space. In this case the results obtained are compared to those presented by Endo et al. (1984).

Composite Rotor

The thin-walled composite shaft, first studied by Zinberg and Symmonds (1970) is made of boron-epoxy with the following characteristics: density $\rho = 1965\,\mathrm{kg/m^3}$, elastic properties $E_1 = 2.11\ 10^{11}\,\mathrm{Pa}$, $E_2 = 2.41\ 10^{10}\,\mathrm{Pa}$, $G_{12} = G_{13} = G_{23} = 6.9\ 10^9\,\mathrm{Pa}$, major Poisson's ratio $\nu_{12} = 0.36$. The shaft length is $L = 2.47\,\mathrm{m}$ and its mean radius is $R = 0.127\,\mathrm{m}$. The thickness, $e = 1.32\ 10^{-3}\,\mathrm{m}$, consists of ten layers of $1.32\,10^{-4}\,\mathrm{m}$ whose orientation are [90°, +45°, −45°, $0°_6$, 90°] given from the inner to the outer surface of the cylinder.

Only 1/6th (60°) of the whole structure is meshed using 4 elements along the circumference and 40 elements along the length. The resulting mesh consists of 160 elements, 1138 nodes, and, consequently, 2809 degrees of freedom.

Two possible values for the critical speed have been obtained by Zinberg and Symmonds (1970) during their test. One at 5500 rpm, deduced from the first natural frequency of the structure at rest ($f_1 = 91.7\,\mathrm{Hz}$) and the other at about 6000 rpm extrapolated from measures performed under rotation. As in the case of this rotor gyroscopic effects are very low, these two values should have been very close.

Considering numerical published studies, Zinberg and Symmonds (1970), Bert and Kim (1995), Singh and Gupta (1996) used an equivalent beam modulus approach, Singh and Gupta (1996) considered also a beam approach derived from a layer wise shell theory and Bert and Kim (1995) used a thin shell approach. The critical speeds obtained using these models are given in Table I, where they are compared to the critical speed computed. Results presented by Dos Reis et al. (1987b), based on Donnell shell theory, which is not adapted to long shells, are not reported here.

The value obtained is coherent with the experimental results and very close to the majority of the results computed on this test case. As the shaft is thin-walled and long, thickness shear deformations should have little effect and classical laminate and beam theories are valid and well adapted.

TABLE I Comparison of the critical speeds calculated using different approaches

Zinberg and Symmonds	1970	Beam	5780 rpm
Bert and Kim	1995	Beam	5788 rpm
Singh and Gupta	1996	Beam	5747 rpm
Singh and Gupta	1996	Beam Shell	5620 rpm
Bert and Kim	1995	Shell	5872 rpm
Present approach		Shell	5776 rpm

Considering the structure at rest the first frequency computed, 96 Hz, is about 5% greater than the published measured value of 91.7 Hz. This result is fully coherent, as for the numerical model boundary conditions are supposed to be perfect.

Short Cylinder—Simply Supported Configuration at Rest

This second test case considers a cylinder, simply supported at both ends, with the following characteristics: length $L = 0.2\,\mathrm{m}$, mean radius $R = 0.1\,\mathrm{m}$ and wall thickness $e = 4\ 10^{-3}\,\mathrm{m}$. The material characteristics are: $\rho = 1600\,\mathrm{kg/m^3}$, $E_1 = 7\ \ 10^{10}\,\mathrm{Pa}$, $E_2 = 2.8\ \ 10^9\,\mathrm{Pa}$, $G_{12} = G_{13} = 1.4\,10^9\,\mathrm{Pa}$, $G_{23} = 5.6\ 10^8\,\mathrm{Pa}$ and $\nu_{12} = 0.25$. The cylinder is constituted by 4 layers of equal thickness and their orientation is [90°, 0°, 90°, 0°].

Three different models are considered. Model 1: discretisation of the whole cylinder using 60×4 elements (60 elements along the circumference and 4 elements along the length). Model 2: discretisation of 1/6th (60°) of the cylinder using 10×4 elements (Figure 2). Model 3: discretisation of 1/12th (30°) using 5×4 elements (Figure 2). Whatever the model, the size of each element is identical. Model 1, computed without reduction using a general purpose in-house finite element code, is considered as a reference. Models 2 and 3 are computed using the proposed

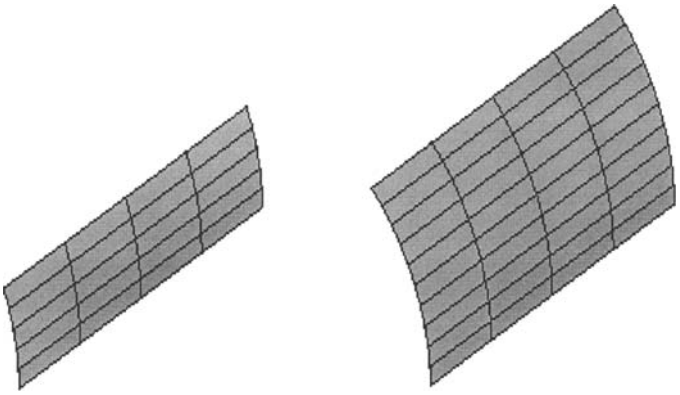

FIGURE 2 Cyclic symmetric sector meshes Model 2: 30° – Model 3: 60°.

TABLE II Short cylinder, frequencies in Hertz computed using models 1, 2 and 3

Mode	Model 1 (full)	Model 2 (60°)	Model 3 (30°)
3*D*	952.6	952.7	952.7
2*D*	1049.2	1049.4	1049.2
4*D*	1284.0	1284.2	1284.1

procedure. Compared to model 1, the number of degrees of freedom involved is divided by a factor of 2.8 for model 2 and 5.3 for model 3.

The results obtained for the first frequencies, which are associated with ring-type modes characterized by nodal diameters (D), are reported in Table II.

As shown in Table II, results are in perfect agreement and this agreement remains unchanged for higher modes. The first frequency can be also compared to the analytical results given by Sun et al. (1997) and obtained from an extended Sanders' shell theory.

Sun et al.	953.1 Hz
Present approach	952.7 Hz

Here again results are in perfect agreement.

Short Cylinder—Free Configuration Under Rotation

Considering the effect of rotation, the proposed approach can be validated by comparison of the results obtained with those given by the classical ring theory.

$$\frac{\omega_n}{p_n} = \frac{2n}{n^2+1}\left(\frac{\Omega}{p_n}\right) \pm \sqrt{1+\frac{n^2(n^2-1)^2}{(n^2+1)^2}\left(\frac{\Omega}{p_n}\right)^2} \qquad [10]$$

where ω_n is the frequency of the rotating structure, p_n is the corresponding frequency at rest, Ω is the rotation speed and n is the wave order directly associated with the number of diameters. Other expressions, which take also into account the gyroscopic effect as well as the effect of large deformations due to rotation, have been proposed. However, expression [10] has been preferred because validated by Endo et al. (1984) against experimental results. Expression [10] is fully valid for a totally free configuration. Consequently, this test case considers the same cylinder as previously but here with free-free boundary conditions. Results computed are reported in Figure 3 for $n=2$ and in Figure 4 for $n=3$.

Frequencies are given with respect to the rotating frame. Then, the lower curves are associated with forward travelling waves while the upper curves are associated with backward travelling waves.

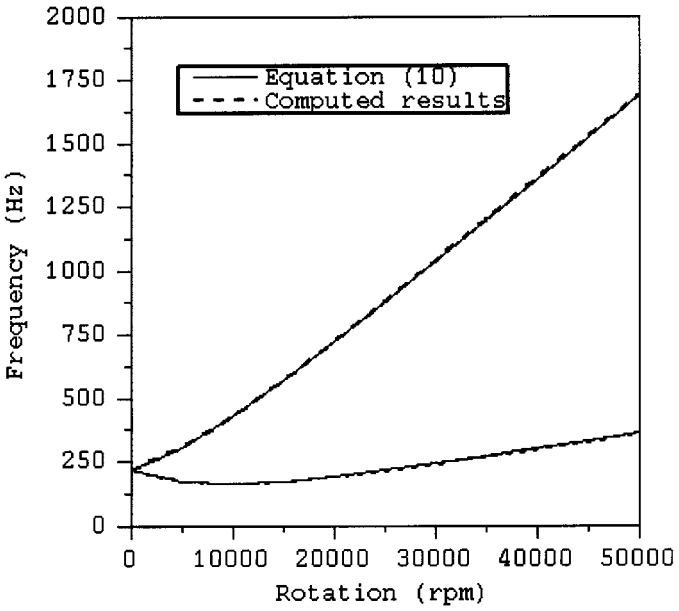

FIGURE 3 Short cylinder free in space. Evolution of frequencies with rotation for $n=2$.

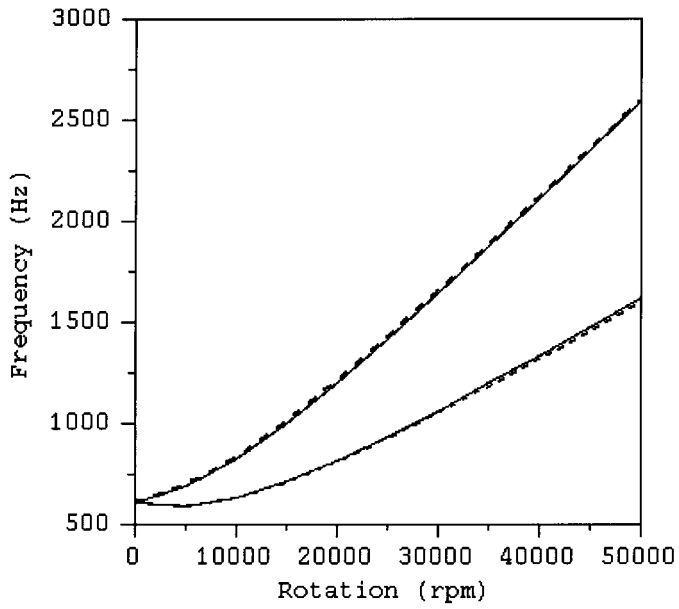

FIGURE 4 Short cylinder free in space. Evolution of frequencies with rotation for $n=3$.

APPLICATION TO A SIMPLE DISC-SHAFT ASSEMBLY

The proposed approach can be applied to isolated shafts or cylinders as shown previously. This approach can also deal with disc-shaft or wheel-shaft assemblies and is able to model couplings that can occur between the different

flexible parts of the assembly. Couplings, mainly induced by inertial effects, are significant for modes associated with $n=0$ and $n=1$. Disc modes with 0 nodal diameter are characterized by a resultant axial force and interact with longitudinal shaft deformations. Disc modes with 1 nodal diameter exert a net pitching moment and a shearing force and interact with shaft bending modes.

The disc-shaft assembly considered is presented in Figure 5. The disc, fixed in an overhung position, is constituted by 8 blades mounted on a circular plate. The outer radius of the disc is $R=0.2$ m and its thickness is $e=3.5\ 10^{-3}$ m. The blade length is $l=0.07$ m. The characteristics of the shaft are: outer radius $r=0.025$ m, wall thickness $h=2\ 10^{-3}$ m, length $L=0.8$ m and overhung length $d=0.1624$ m.

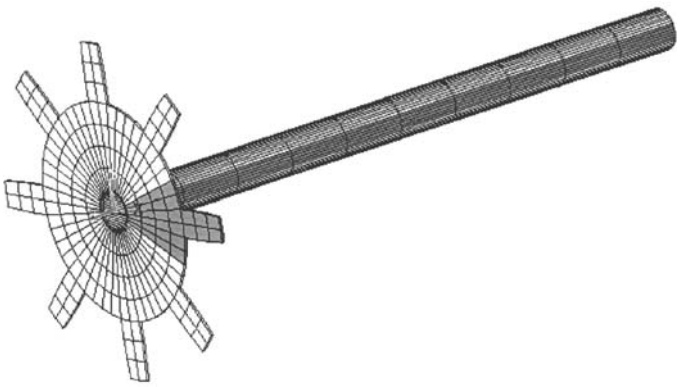

FIGURE 5 Disc shaft assembly. Only 1/8th of the mesh (dark portion) is considered by the numerical model.

Two different materials are considered steel ($\rho=7800$ kg/m^3, $E_1=E_2=2.1\ 10^{11}$ Pa, $G_{12}=G_{13}=G_{23}=8.07\ 10^{10}$, $\nu=0.3$) and graphite epoxy ($\rho=1578$ kg/m^3, $E_1=1.39\ 10^{11}$ Pa, $E_2=1.1\ 10^{10}$ Pa, $G_{12}=G_{13}=6.1\ 10^{9}$ Pa, $G_{23}=3.8\ 10^{9}$ Pa and $\nu_{12}=0.3$). The disc is made of steel and the shaft is constituted by 10 graphite–epoxy layers of equal thickness with the following orientations [90°, +45°, −45°, $0°_6$, 90°].

The influence of disc flexibility on the overall behavior is pointed out by comparing the results given by two different models. The first considers disc flexibility while the second one is a rigid disc model, simply obtained by multiplying the Young's modulus associated with each disc element by 10 000. A portion of 1/8th (45°) of the whole assembly is meshed using multilayered shell elements for the shaft and isoparametric elements with 20 nodes for the disc. The resulting mesh, reduced to the dark zone shown in Figure 5, comprises 711 nodes and consequently 1848 degrees of freedom.

The progression of frequencies with rotation is presented in Figure 6. For clarity, only the first modes are reported. At rest, mode shapes are classified as follows: the first is a first shaft bending mode ($1F$) and the second is a disc mode with one nodal diameter ($1D$). This classification is based on the main component of mode shapes, which are in fact highly coupled disc-shaft modes, as shown in Figure 7 for the second mode.

The influence of disc flexibility at rest is quantified in Table III, which confirms the coupled nature of mode shapes.

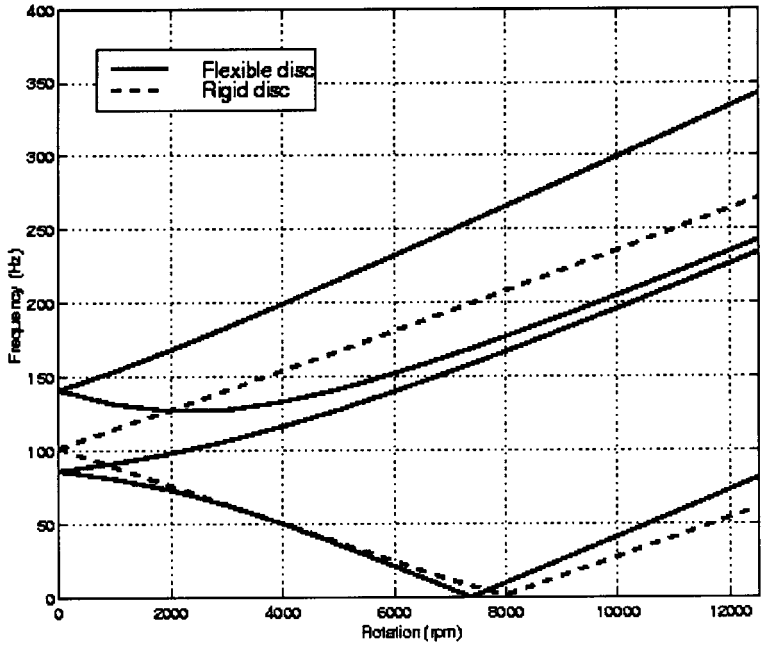

FIGURE 6 Evolution of frequencies with rotation, rotating frame. Influence of disc flexibility.

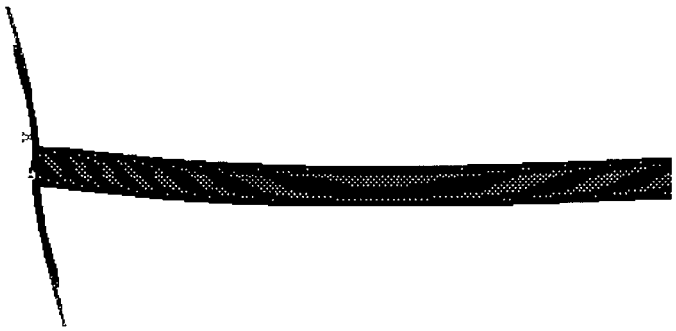

FIGURE 7 Second mode shape at rest (141.2 Hz).

TABLE III Disc-shaft assembly. Frequencies at rest (Hertz)

Mode	Flexible disc	Rigid disc	Δ
1*F*	86.1	101.6	18%
1*D*	141.2	–	

Considering the progression of shaft frequencies with rotation, the forward branch (lower branch in the rotating frame) is less influenced by disc flexibility effects than the backward branch. The difference between the critical speeds predicted by the flexible disc and rigid disc models is about 8.4%.

CONCLUSION

This paper presents a numerical technique for the calculation of natural frequencies and mode shapes of composite rotors. This technique, based on a three dimensional finite element discretisation of the assembly, can deal with bending or torsional shaft modes, as well as with ring type modes of thin-walled tubes or disc-shaft couplings. The computational effort needed is kept acceptable by using efficient reductions. First, a modal reduction, based on mode shapes at rest, is used to calculate the behavior of the rotating structure and the whole disc-shaft assembly is supposed to be cyclically symmetric.

The application to a composite rotor, often considered as a reference test case in the literature, and to a short cylinder illustrates and validates the proposed method. Finally, the results obtained on a simple disc-shaft assembly show the effects of possible couplings between shaft and disc deformations. The highly coupled nature of the first shaft bending mode and the disc mode with one nodal diameter is clearly highlighted.

NOMENCLATURE (S.I. UNITS)

$[M]$	mass matrix
$[CM]$	mechanical damping matrix
$[CR]$	gyroscopic matrix
$[KE]$	elastic stiffness matrix
$[KG]$	geometric stiffness matrix (stress stiffening)
$[KS]$	supplementary stiffness matrix (spin softening)
$\{FC\}$	modal centrifugal forces vector
$\{\delta\}_s$	static equilibrium position under centrifugal loading
$\{\delta\}_d$	small amplitude dynamic displacement around the static position
$\{\delta\}_d^p$	dynamic displacement of sector p
$\{\delta_n^c\}$	generalized quantities associated with the basic sector
$\{\delta_n^s\}$	generalized quantities associated with the basic sector
N	total number of identical jointed sectors (cyclic symmetry)
n	Fourier order (wave order) directly associated with the number of diameters
$\beta_n = 2\pi n/N$	phase difference between the displacement of two adjacent sectors
$[\Psi_n]$	modal matrix
$\{q_n\}$	generalized coordinates
$[m_n] = [\Psi_n]^t[M_n][\Psi_n]$	generalized mass matrix
$[c_n] = [\Psi_n]^t[CM_n + CR_n][\Psi_n]$	generalized damping matrix
$[k_n] = [\Psi_n]^t[KE_n + KG_n - KS_n][\Psi_n]$	generalized stiffness matrix
ω_n	frequency of the rotating structure
p_n	corresponding frequency at rest
Ω	rotation speed

REFERENCES

Ahmad, S., Zienkiewicz, O. C., and Irons, B. (1970) Analysis of Thick and Thin Shell Structures by Curved Finite Elements, *International Journal for Numerical Methods in Engineering*, **2**, 419–451.

Bauchau, O. A. (1983) Optimal Design of High Speed Rotating Graphite/Epoxy Shafts, *Journal of Composite Materials*, **17**(3), 170–181.

Bert, C. W. and Kim, C. D. (1995) Whirling of Composite-Material Driveshafts including Bending-Twisting Coupling and Transverse Shear Deformation, *Journal of Vibration and Acoustics*, **117**(1), 17–21.

Chen, Y., Zhao, H. B., and Shen, Z. P. (1993) Vibrations of High Speed Rotating Shells with Calculations for Cylindrical Shells, *Journal of Sound and Vibration*, **160**(1), 137–160.

Darlow, M. S. and Creonte, J. (1995) Optimal Design of Composite Helicopter Power Transmission Shafts with Axially Varying Fiber Layup, *Journal of the American Helicopter Society*, **40**(2), 50–56.

Dos Reis, H. L. M. and Goldman, R. B. (1987a) Thin Walled Laminated Composite Cylindrical Tubes: Part I Boundary Value Problems, Part II Bending Analysis, *Journal of Composite Technology and Research*, **9**, 47–57.

Dos Reis, H. L. M., Goldman, R. B., and Verstrate, P. H. (1987b) Thin Walled Laminated Composite Cylindrical Tubes: Part III Critical Speed Analysis, *Journal of Composite Technology and Research*, **9**, 58 – 62.

Endo, M., Hatamura, K., Sakata, M., and Taniguchi, O. (1984) Flexural Vibration of a Thin Rotating Ring, *Journal of Sound and Vibration*, **92**(2), 261 – 272.

Gupta, K. and Singh, S. P. (1998) Damping Measurements in Fiber Reinforced Composite Rotors, *Journal of Sound and Vibration*, **211**(3), 513 – 520.

Jacquet-Richardet, G. and Swider, P. (1997) Influence of Fiber Orientation on the Dynamic Behavior of Rotating Laminated Composite Blades, *Communications in Numerical Methods in Engineering*, **13**, 815 – 824.

Jacquet-Richardet, G., Ferraris, G., and Rieutord, P. (1996) Frequencies and Modes of Rotating Flexible Bladed-Disc-Shaft Assemblies: A Global Cyclic Symmetry Approach, *Journal of Sound and Vibration*, **191**(5), 901 – 915.

Lam, K. Y. and Loy, C. T. (1995) Analysis of Rotating Laminated Cylindrical Shells by Different Thin Shell Theories, *Journal of Sound and Vibration*, **186**(1), 23 – 35.

Padovan, J. (1975) Traveling Waves Vibrations and Buckling of Rotating Anisotropic Shells of Revolution by Finite Elements, *International Journal of Solids Structures*, **11**, 1367 – 1380.

Singh, S. P., Gubran, H. B. H., and Gupta, K. (1997) Development in Dynamics of Composite Material Shafts, *International Journal of Rotating Machinery*, **3**, 189 – 198.

Singh, S. P. and Gupta, K. (1996) Composite Shafts Rotordynamic Analysis using a Layerwise Theory, *Journal of Sound and Vibration*, **191**(5), 739 – 756.

Singh, S. P. and Gupta, K. (1994a) Free Damped Flexural Vibration Analysis of Composite Cylindrical Tubes Using Beam and Shell Theories, *Journal of Sound and Vibration*, **172**(2), 171 – 190.

Singh, S. P. and Gupta, K. (1994b) Damped Free Vibrations of Layered Composite Cylindrical Shells, *Journal of Sound and Vibration*, **172**(2), 191 – 209.

Sivadas, K. R. and Ganesan, N. (1994) Effect of Rotation on Vibration of Moderately Thick Circular Cylindrical Shells, *ASME Journal of Vibration and Acoustics*, **116**(2), 198 – 202.

Smirnov, A. (1989) Free Vibrations of the Rotating Shells of Revolution, *ASME Journal of Applied Mechanics*, **56**(2), 423 – 429.

Stephenson, R. W. and Rouch, K. E. (1993) Modeling Rotating Shafts using Axisymmetric Solid Finite Elements with Matrix Reduction, *ASME Journal of Vibration and Acoustics*, **115**(4), 485 – 489.

Sun, G., Bennett, P. N., and Williams, F. W. (1997) An Investigation on Fundamental Frequencies of Laminated Circular Cylinders Given by Shear Deformable Finite Elements, *Journal of Sound and Vibration*, **205**(3), 265 – 273.

Thomas, D. L. (1979) Dynamics of Rotationally Periodic Structures, *International Journal for Numerical Methods in Engineering*, **14**, 81 – 102.

Zinberg, H. and Symmonds, M. F. (1970) The Development of on Advanced Composite Tail Rotor Driveshaft, *Proceeding of the 26th Annual National Forum of American Helicopter Society*, Washington DC.

Zorzi, E. S. and Giordano, J. C. (1985) Composite Shaft Rotordynamic Evaluation, ASME paper Vol. 85-det-114. *ASME Design. Engineering Division Conferences in Mechanical Vibration and noise*. Cincinnati USA.

APPENDIX

Considering a reference cyclic symmetric sector of the whole assembly, the associated matrices obtained after finite element discretisation can be partitioned into three blocks linked to the left boundary (l), right boundary (r) and interior (i) degrees of freedom. For example, this repartition gives, for the mass matrix:

$$[M] = \begin{vmatrix} M_{ll} & M_{li} & M_{lr} \\ M_{il} & M_{ii} & M_{ir} \\ M_{rl} & M_{ri} & M_{rr} \end{vmatrix}$$

Accordingly, matrices in Eq. (8) $[m_n]$ is a diagonal matrix, $[c_n]$ is a non-diagonal anti-symmetric matrix and $[k_n]$ is a full matrix can be expressed as:

$$\begin{bmatrix} M_{ll} + M_{rr} + (M_{lr} + M_{rl})\cos\beta & M_{li} + M_{ri}\cos\beta & (M_{lr} + M_{rl})\sin\beta & -M_{ri}\sin\beta \\ M_{il} + M_{ir}\cos\beta & M_{ii} & M_{ir}\sin\beta & 0 \\ (M_{rl} + M_{lr})\sin\beta & M_{ri}\sin\beta & M_{ll} + M_{rr} + (M_{lr} + M_{rl})\cos\beta & M_{li} + M_{ri}\cos\beta \\ -M_{ir}\sin\beta & 0 & M_{il} + M_{ir}\cos\beta & M_{ii} \end{bmatrix}$$